Electronic Supplementary Material (ESI) for Materials Chemistry Frontiers.

Supplementary Information

Structure-property relationship on insertion of Fluorine *versus* Nitrogen-substituents in wide bandgap polymer donors for non-fullerene solar cells: An interesting case study

Gururaj P. Kini, Yong Woon Han, Sung Jae Jeon and Doo Kyung Moon*

Nano and Information Materials (NIMs) Laboratory,

Department of Chemical Engineering,

Konkuk University, 120, Neungdong-ro, Gwangjin-gu, Seoul 05029, Korea.

Experimental section

1.1 General Information:

Nuclear magnetic resonance (NMR) spectra were analyzed on a Bruker ARX 400 spectrometer instrument operating at 400 MHz for ^{1}H NMR and operating at 100 MHz for ^{13}C NMR. UV-vis absorption measurements were carried out with HP Agilent 8453 UV-Vis spectrophotometer with a wavelength range of 300-900 nm. All solution UV-vis experiments were measured in chloroform (CF) solutions and films were prepared by spin-coating CF solutions onto quartz substrates. The molar absorption coefficients (ε) of the NFAs were calculated from the UV–vis data on chloroform solutions with different concentrations of the order 10^{-4} M and the Beer–Lambert equation. For the sample of thin films, the films were prepared by spin-coating (3000~4000 rpm) (15 mg/mL for neat films in chloroform solution (Film thickness ~90 and 80 nm for P1-2F and P2-2N), 22 mg/mL for blend films in chlorobenzene/0.5 vol% DIO solutions (Thickness ~110 and 100 nm, for P1-2F and P2-2N-based blend film, respectively) on quartz plates. The absorption coefficients of the polymer films were obtained by dividing the absorbance by the film thickness. To measure the thickness of thin films, several grooves were firstly marked on the thin film by a pointed tweezer, and then the depths of the grooves were recorded on Alpha step surface profiler ET200. The average value of the depths was used as the thickness of the thin film. Cyclic voltammograms (CV) were determined by using a Zahner IM6eX electrochemical workstation and at a scan rate of 50 mVs^{-1} at 25 ^{o}C under argon using 0.1 M tetra butyl ammonium hexafluorophosphate (Bu_4NPF_6) in acetonitrile as the electrolyte. During measurement of CV, Pt wire was used as the counter electrode, Ag/AgCl electrode [Ag in 0.1 M KCl] was used as the reference electrode and polymer was drop cast on a carbon electrode used as the working electrode. The electrochemical potential was calibrated against the ferrocene/ferrocenium (Fc/Fc^{+}) system. The highest occupied molecular orbital (HOMO) levels of the polymers were determined using the oxidation onset value. At the same time, LUMO levels were calculated from the equation LUMO = E_g^{opt} – HOMO (where E_g^{opt} is the optical bandgap of polymer from the thin film state). Thermogravimetric analysis (TGA) measurements were performed on a NETZSCH TG 209 F3 thermogravimetric analyzer, where samples were run under N_2 and heated from room temperature to 400 °C at a rate of 10 °C/min. All gel permeation chromatography (GPC) analyses were performed using CF as an eluent and a

polystyrene standard as a reference. X-ray diffraction (XRD) patterns were obtained using a Smart Lab 3 kW (40 kV 30 mA, Cu target, 1.541 Å) instrument of Rigaku, Japan. The Photoluminescence (PL) spectra were taken on a Perkin Elmer LS55 spectrometer. Firstly, to analyze the extent of photo-induced electron transfer, both the polymer and blends were excited at 530 nm and the corresponding PL emission spectrum was recorded. Similarly, the PL emission spectrum of pristine IT-4F and blend films were obtained by exciting at 700 nm to evaluate hole transfer efficiency. PL quenching efficiency was calculated according to the equation: $\Delta PL = 1 - PL_{blend}/PL_{polymer} \times 100$, where PL_{blend} and $PL_{polymer}$ are the PL intensity of the blend and neat polymer films, respectively.[1] Atomic force microscopy (AFM) measurements of size (2×2 μm^2) were obtained using a scanning probe XE-100 in a tapping mode. TEM images were obtained on JEM-2100F instrument. The active layer films for the TEM measurements were spin-coated onto ITO/PEDOT:PSS substrates, and then these substrates with the active layers were submerged in deionized water to make the active layers fall off, then the active layer films were picked up by copper grids for TEM measurements.

1.2 Fabrication and characterization of PSCs:

All the BHJ photovoltaic cells were prepared using an inverted device fabrication procedure. Indium tin oxide (ITO) glass (10 Ω sq^{-1}, Samsung corning) was sequentially sonicated for a period of 10 min in order, detergent (Alconox in deionized water), acetone, isopropyl alcohol, and deionized water. To ensure the complete removal of the remaining water, the ITO glass was heated on a hot plate for 10 min at 120 °C. For the hydrophilic treatment of the ITO glass surface, the glass was cleaned for 15 min in a UVO cleaner. Then zinc oxide (ZnO) sol-gel precursor[2] in 2-methoxy ethanol was spin-coated onto the UVO-treated ITO to produce a 10 nm thick layer by spin-coating at 3000 rpm. The coated glass was then dried at 200 °C for 60 min on the hot plate. Composite solutions of the polymer and IT-4F were prepared using CB and 0.5 vol% DIO (optimal donor and acceptor weight ratios of 1:1.1 for P1-2F:IT-4F and P2-2N:IT-4F blends with a total concentration of 22 mg mL^{-1}) were filtered through a 0.5 μm polytetrafluoroethylene (PTFE) filter and then spin-coated (1000 - 4000 rpm, 30 s) on top of the ZnO layer. Then, the active layer was set above the hot plate at 130 °C for 10 mins for thermal annealing and then cooled to room temperature. Finally, inverted device fabrication was completed by depositing thin layers MoO_3 (5 nm) and Ag (100 nm) in a vacuum (10^{-6} torr) using a thermal evaporator. The current density–

voltage (J–V) characteristics of the devices were measured using a Keithley 2400 source meter. The light source used a solar simulator (Oriel). The output photocurrent was adjusted to match the photocurrent of the Si 4 reference cell to obtain a power density of AM 1.5G 100 mW cm^{-2}. The external quantum efficiency (EQE) characteristics were measured using an IPCE measurement system (Mcscience, Polaronix K3100).

1.3 Charge measurements:

The charge-carrier mobility of polymer:IT-4F blends was measured by using the space-charge limited current (SCLC) technique method. The hole only (ITO/PEDOT:PSS/active layer/MoO_3/Ag) and electron-only device (ITO/ZnO/active-layer/PDINN/Ag) devices were fabricated with optimum blend ratios in CB:DIO (0.5 vol% DIO). The charge carrier mobility was determined by fitting dark *J-V* measurements results in the 0-5 V range into space charge limited form and mobility (μ) calculated using Mott–Gurney equation $J = 9\varepsilon_0\varepsilon_r\mu V^2/8L^3$, where μ = charge carrier mobility, J = current density, ε_r = dielectric constant of the polymer and assumed to be 3,[3-5] ε_0 = permittivity of free space (8.85×10^{-14} F cm^{-1}), L = active layer thickness (110 and 100 nm, for P1-2F and P2-2N-based blend film, respectively) and V (= V_{appl} - V_{bi}) is the internal voltage in the device, where V_{appl} is the applied voltage to the device and V_{bi} is the built-in voltage due to the relative work function difference of the two electrodes. The mobility μ was determined by fitting the dark current to the model of a single carrier SCLC, which is described by the equation above.

1.4 Materials and Methods.

All chemicals and solvents were purchased from Aldrich, Alfa Aesar and TCI Chemical Co. companies and used as received. The synthetic routes of monomers and polymers are given in Figure 1 in the main manuscript. The monomers 2FBn-Br **(M1)** and Pz-Br **(M2)** were prepared from the commercially available cheap starting materials 1,4-dibromo-2,5-difluorobenzene (1) and 2,5-dibromopyrazine (2) in simple two steps as reported in our previous report.[6, 7] and Cl-BDT-Sn was purchased from the Suna Tech.

General procedure for the synthesis of intermediate 4 or 5:

A mixture of tributyl(4-(2-ethylhexyl)thiophen-2-yl)stannane (3) (3 eq), 1,4-dibromopyrazine (**1**) or 2,5-dibromopyrazine (2) (1 eq), and tetrakis(triphenylphosphine)palladium(0) (5 mol%) in

toluene (25vol) was degassed twice with nitrogen (N2). The reaction mixture was then heated at 110 °C for 24 h; after cooling, the mixture was poured into water (100 mL) and extracted with chloroform. The organic layer was dried over anhydrous MgSO4. The crude compound was purified by silica gel chromatography with dichloromethane (30%) in hexane.

5,5'-(2,5-difluoro-1,4-phenylene)bis(3-(2-ethylhexyl)thiophene) (4): (0.58 g, yield 82%) as gummy colorless liquid. **^{1}H NMR (400 MHz, $CDCl_3$, δ ppm):** 7.36 (t, 2H, J = 9.3 Hz), 7.30 (s, 2H), 6.95 (s, 2H), 2.56 (d, 4H, J = 7.3 Hz), 1.58 (m, 2H), 1.34-1.28 (m, 16H) and 0.88 (t, 6H, J = 7.6 Hz). **^{13}C NMR (100MHz, $CDCl_3$, δ ppm):** 156.07, 153.62, 142.95, 135.26, 128.73, 128.71, 128.68, 122.09, 114.93, 40.31, 34.58, 32.48, 28.89, 25.62, 23.06, 14.16, 10.85.

2,5-bis(4-(2-ethylhexyl)thiophen-2-yl)pyrazine (5): (0.34 g, yield 69%), Yellow solid. **^{1}H NMR (400 MHz, $CDCl_3$, δ ppm):** 8.80 (s, 4H), 7.46 (s, 2H), 7.03 (s, 2H), 2.58 (d, J = 6.87 Hz, 4H), 1.60 (m, 2H), 1.35-1.27 (m, 16H) and 0.89 (m, 12H). **^{13}C NMR (100MHz, $CDCl_3$, δ ppm):**146.01, 143.60, 140.76, 139.40, 127.06, 124.28, 40.32, 34.60, 32.46, 28.88, 25.62, 23.05, 14.15, 10.85.

General procedure for the synthesis of monomer 2FBn-Br (M1) and **Pz-Br (M2):**

To the stirred solution of compound **4** or **5** (1eq) in THF (30 vol), N-Bromosuccinimide (NBS) (2.5 eq) was added at room temperature and the reaction mass was stirred overnight under dark. After cooling, the reaction mass was quenched with sodium bicarbonate solution and extracted with chloroform (50ml x 3). The organic extraction was dried over anhydrous magnesium sulfate and then concentrated. The crude product was purified by silica gel column with dichloromethane (20%) in hexane as eluent to obtain the corresponding brominated product.

5,5'-(2,5-difluoro-1,4-phenylene)bis(2-bromo-3-(2-ethylhexyl)thiophene) (2FBn-Br, M1) (0.64 g, 84%) as off-white solid. **^{1}H NMR (400 MHz, $CDCl_3$, δ ppm):** 7.32 (t, 2H), 7.14 (s, 2H), 2.50 (d, 4H, J = 7.3 Hz), 1.62 (m, 2H), 1.34-1.23 (m, 16H) and 0.90 (m, 6H). **^{13}C NMR (100MHz, $CDCl_3$, δ ppm):** 155.84, 153.87, 142.27, 134.83, 128.16, 121.49, 114.68, 111.61, 40.05, 33.88, 32.51, 28.84, 25.71, 23.15, 14.24, 10.91.

2,5-bis(5-bromo-4-(2-ethylhexyl)thiophen-2-yl)pyrazine (Pz-Br, M2): (0.37 g, yield 81%), Yellow solid. **^{1}H NMR (400 MHz, $CDCl_3$, δ ppm):** 8.72 (s, 4H), 7.29 (s, 2H), 2.52 (d, J = 7.16 Hz, 4H), 1.65 (m, 2H), 1.35-1.27 (m, 16H) and 0.89 (m, 12H). **^{13}C NMR (100MHz, $CDCl_3$, δ**

ppm): 145.38, 142.99, 140.52, 138.87, 126.45, 113.94, 39.97, 33.95, 32.46, 28.77, 25.68, 23.05, 14.13, 10.84.

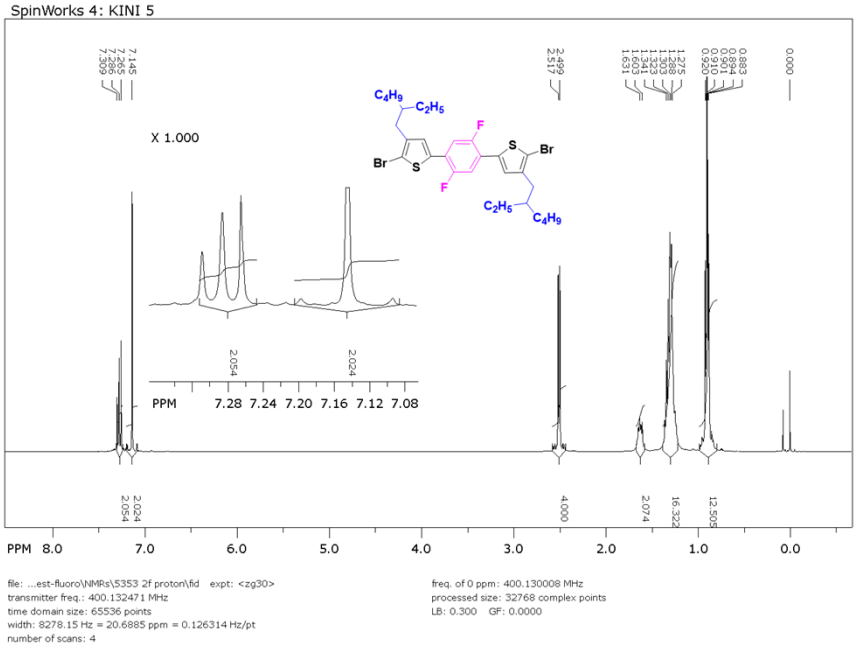

Figure S1 ^{1}H NMR (top) and ^{13}C NMR (bottom) of monomer **M1**.

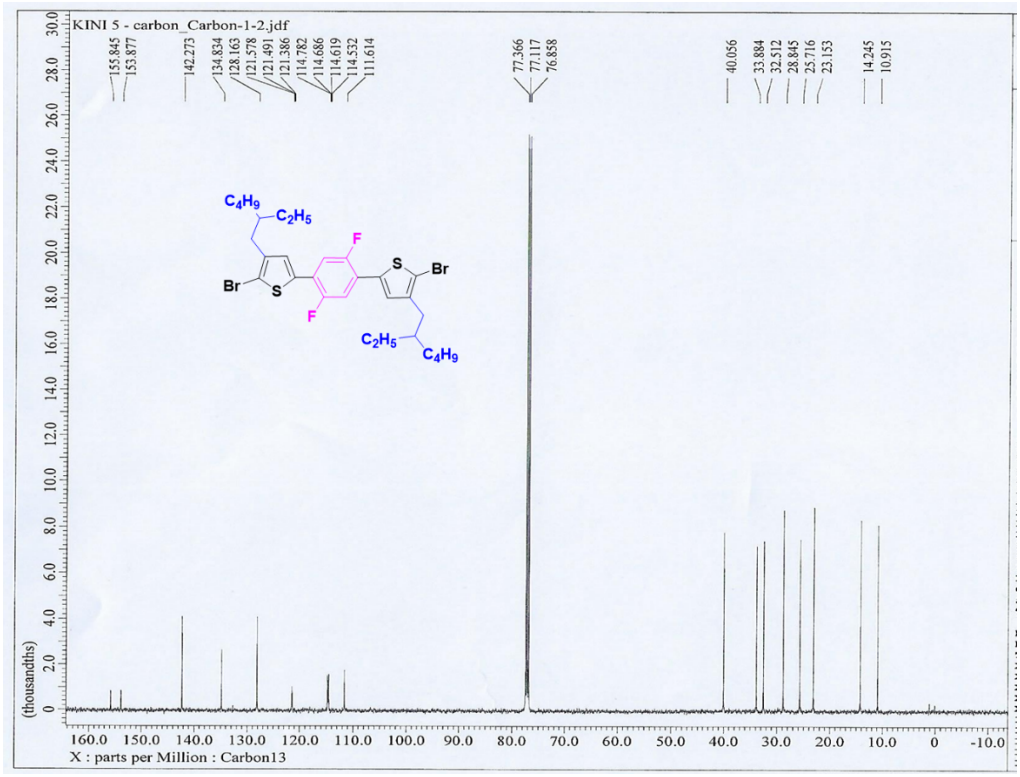

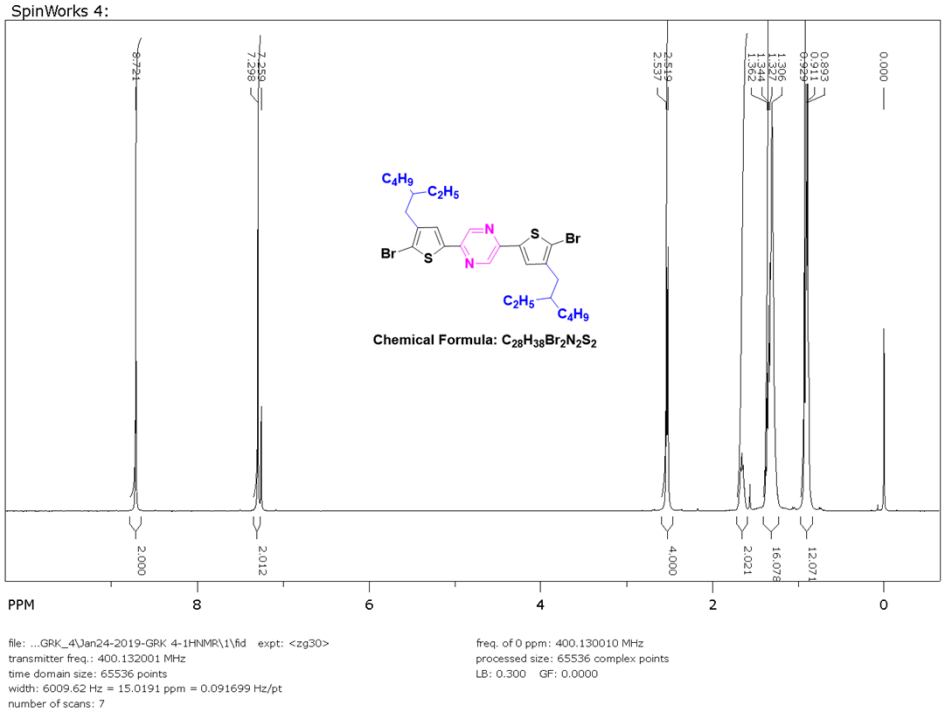

Figure S2 ^{1}H NMR (top) and ^{13}C NMR (bottom) of monomer **M2**.

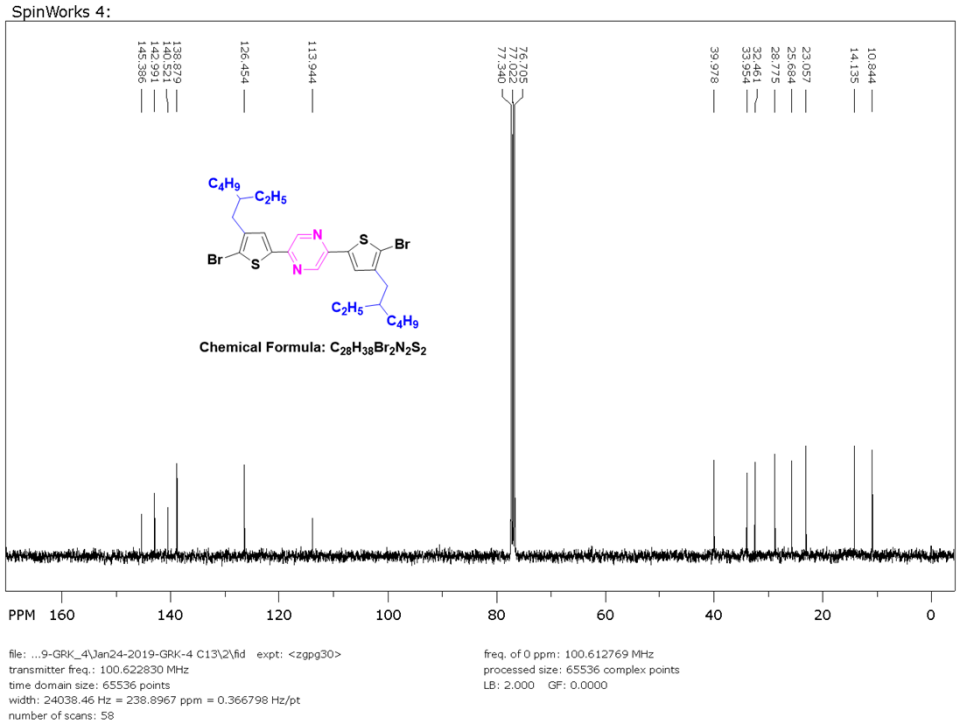

General procedures for synthesizing polymers

To the clean dry 5 mL microwave vial monomer (**M1 or M2**) (0.15 mmol), stannylated BDT monomers (**ClBDT-Sn**) (0.15 mmol), $Pd_2(dba)_3$ (3 mole%), and tri-(o-tolyl)phosphine (6 mole%) were added, followed by 1 mL of anhydrous chlorobenzene. The resulting reaction mixture was subsequently heated at 110 °C for 10 min, 125 °C for 10 min and then 140 °C for 60 min in a microwave reactor. Then polymer was end-capped by the addition of 2-tributylstannylthiophene (0.1 equiv.) and the mixture was further reacted at 145 °C for 20 min. Similarly, 2-Bromothiophene (0.2 equiv.) was added by a syringe and the reaction solution was heated at 145 °C for another 20 min. Then reaction mixture was then cooled to room temperature, and the polymer was precipitated into methanol. Finally, crude precipitated polymer was purified by Soxhlet extraction using methanol for 12h, acetone for 12h, hexane for 12h and chloroform (CF) 12 hours. The CF solution was then concentrated under reduced pressure and precipitated into methanol and filtered to give polymer, which was dried in an oven for 24 h before device fabrication.

Synthesis of poly-{4,8-bis(4-chloro-5-(2-ethylhexyl)thiophen-2-yl)-2-(3-(2-ethylhexyl)-5-(4-(4-(2-ethylhexyl)-5-methylthiophen-2-yl)-2,5-difluorophenyl)thiophen-2-yl)-6-methylbenzo[1,2-b:4,5-b']dithiophene} (P1-2F) (130 mg, 74%) as red solid. The polymer was dried in vacuum oven **GPC analysis**: Mn = 32,255, Mw = 109,667 and PDI = 3.4. $\mathbf{T_d}$ = 431 °C.

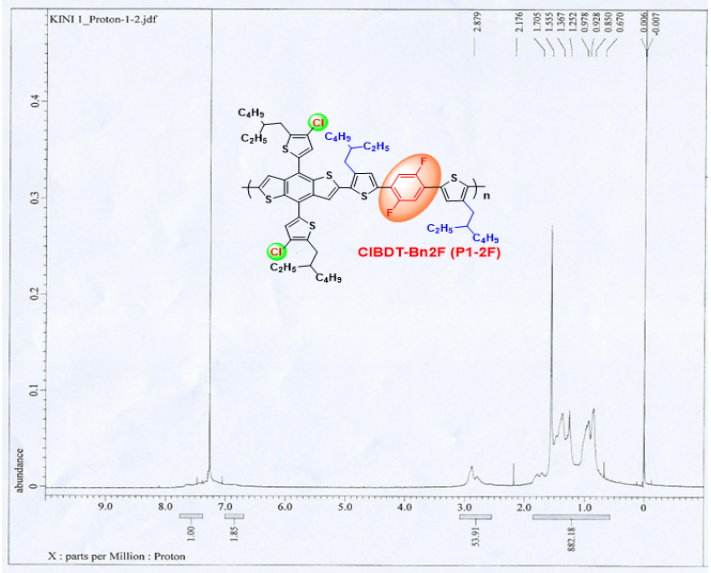

Figure S3. ^{1}H NMR of polymer **P1-2F**.

poly-{2-(5-(4,8-bis(4-chloro-5-(2-ethylhexyl)thiophen-2-yl)-6-methylbenzo[1,2-b:4,5-b']dithiophen-2-yl)-4-(2-ethylhexyl)thiophen-2-yl)-5-(4-(2-ethylhexyl)-5-methylthiophen-2-yl)pyrazine} (P2-2N) (120 mg, 70%) as deep red solid. The polymer was dried in vacuum oven **GPC analysis**: Mn = 30,418, Mw = 94,890 and PDI = 3.11. $\mathbf{T_d}$ = 421 °C.

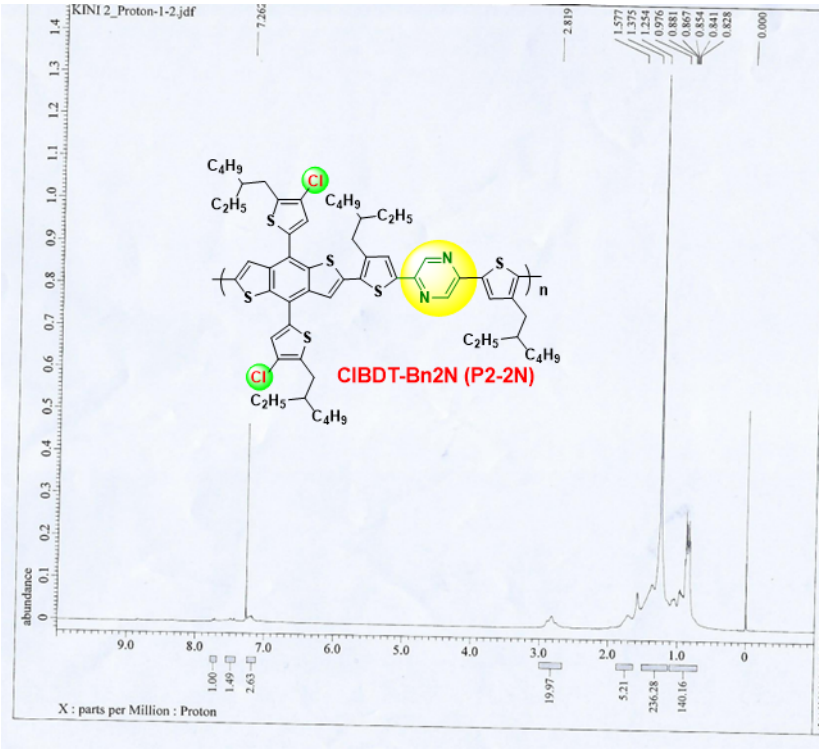

Figure S4. ^{1}H NMR of polymer **P2-2N**.

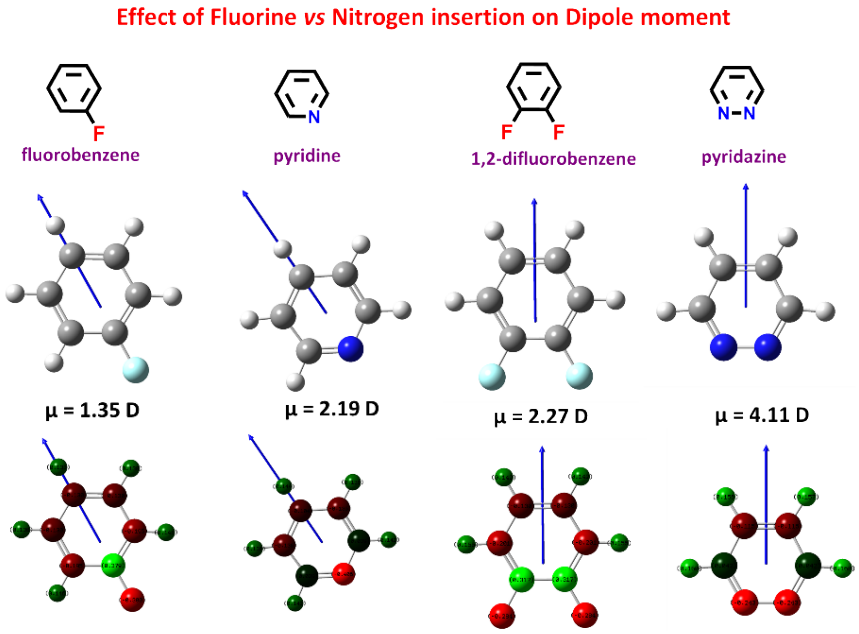

Figure S5. Effect of one or two fluorine and nitrogen insertion on the dipole moment of the molecules predicted using DFT (Calculated using the Gaussian 09 package at the B3LYP/6–31G* level). Color assignment of molecules Grey = carbon, White = hydrogen, Sky blue = fluorine and Dark blue = nitrogen.

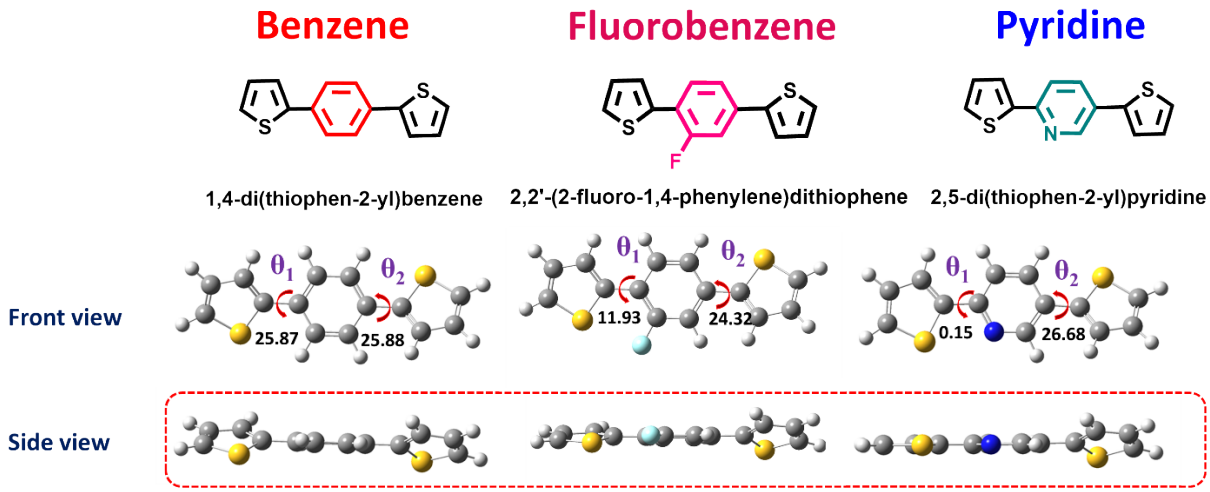

Figure S6. Effect of fluorine and nitrogen insertion on molecular geometry of the molecules predicted using DFT (Calculated using the Gaussian 09 package at the B3LYP/6–31G* level). Color assignment of molecules Grey = carbon, White = hydrogen, Yellow = Sulphur, Sky blue = fluorine and Dark blue = nitrogen.

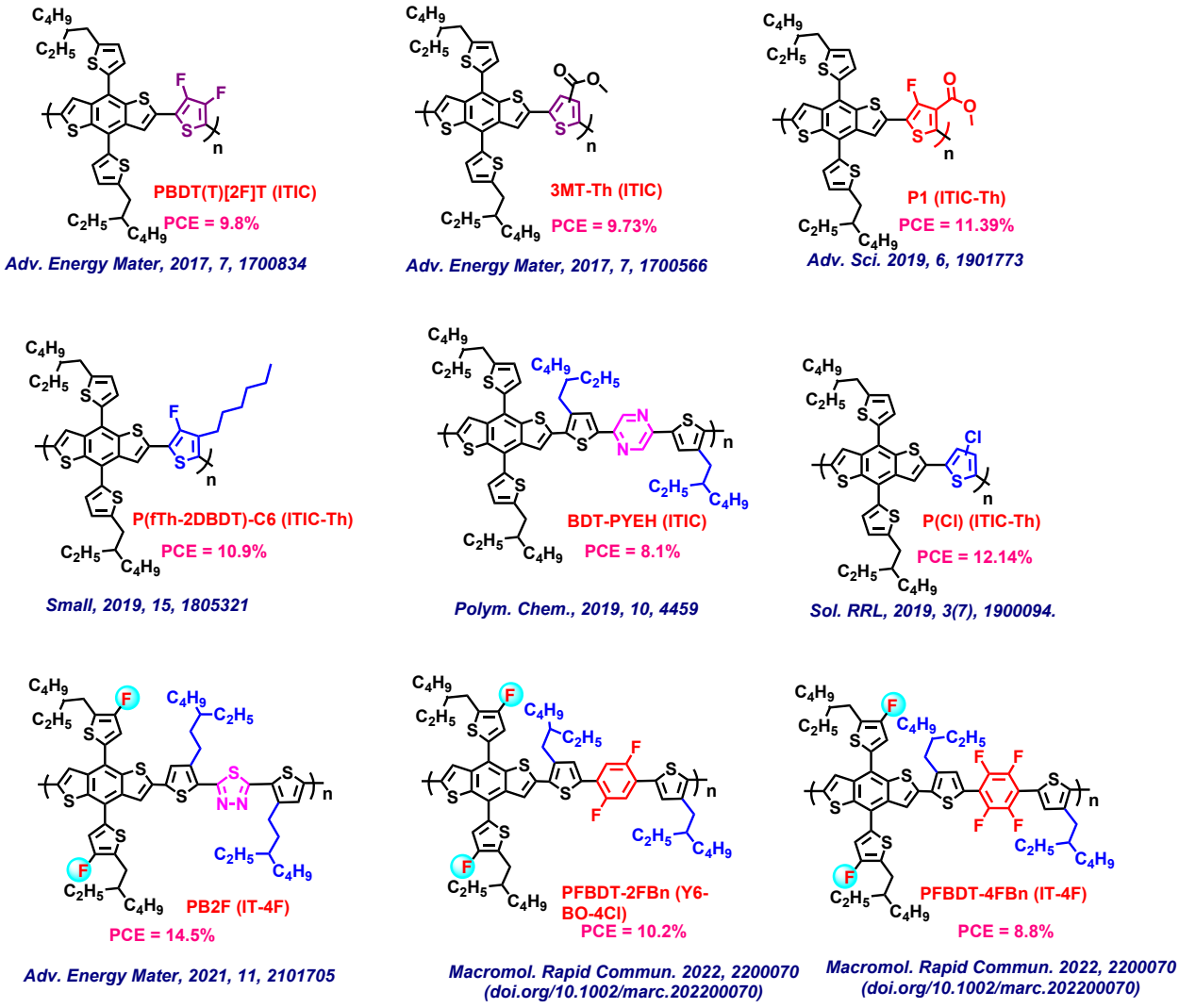

Figure S7. Chemical structures of the representative low-cost donor polymers involving alternate BDT and thiophene and/or heteroarene units with various electron-withdrawing substituents as a weak "A" unit reported in the literature.

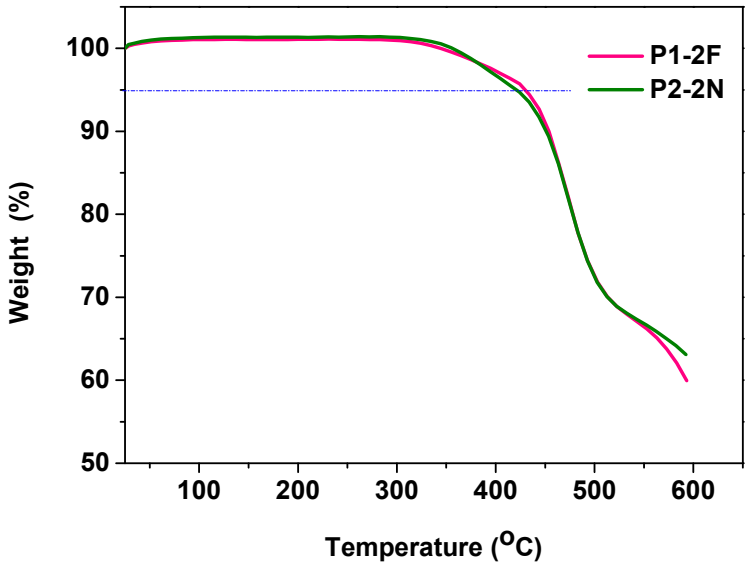

Figure S8. TGA plots of polymers at a heating rate of 10 °C/min under nitrogen atmosphere.

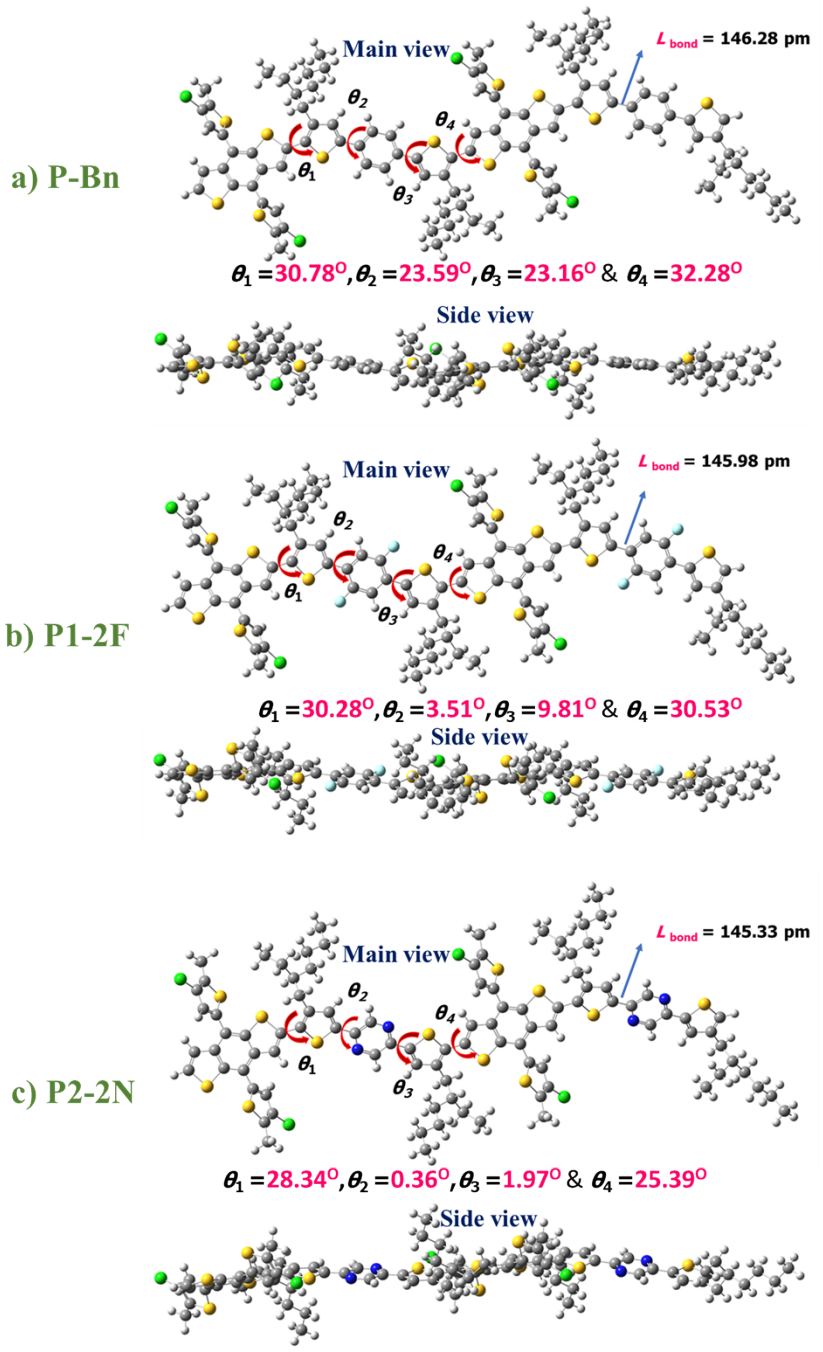

Figure S9. The optimized molecular geometries of polymer (a) **P-Bn** (reference with benzene) (b) **P1-2F** (with 2,5-diflurobenzene) and (c) **P2-2N** (with pyrazine) as acceptor core. (Calculated using the Gaussian 09 package at the B3LYP/6–31G* level).

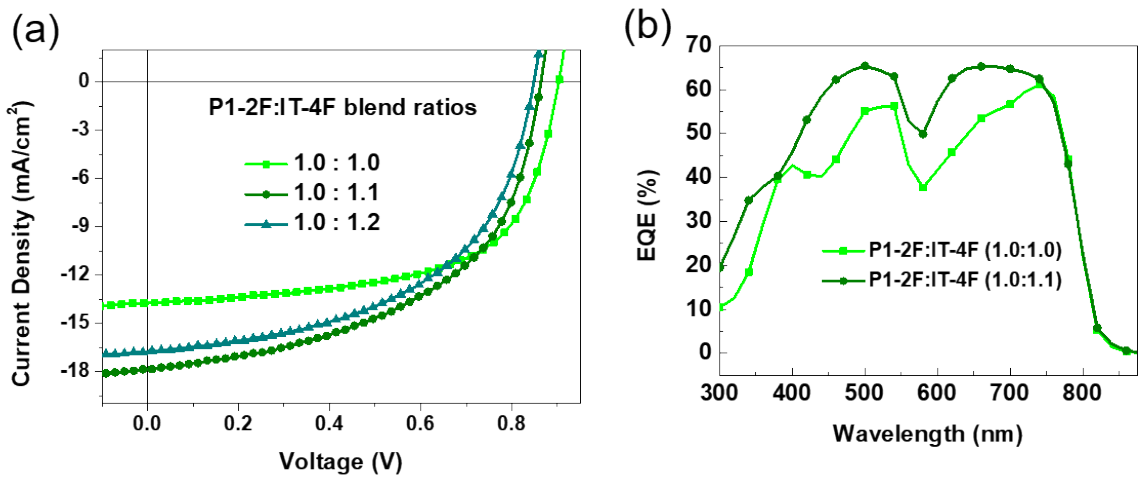

Figure S10 (a) *J-V* characteristics and (b) EQE corresponding profiles **P1-2F**:IT-4F based PSCs with different D:A blend ratios (CB/0.5 vol % DIO) under inverted device architecture ITO/ZnO/active layer/MoO_3/Ag with thermal annealing 140 °C for 10 mins.

Table S1. Device characteristics of **P1-2F**:IT-4F (CB/0.5 vol % DIO) OSCs processed with different blend ratios under optimized device fabrication conditions.

Polymer	**Polymer:IT-4F blend ratio**	**Thermal annealing temperature [°C]**	V_{OC} **[V]**	J_{SC} **[mA/cm²]**	***FF*** **[%]**	**PCE [%]**
P1-2F	**1.0:1.0**	140	0.903	13.7	61.9	7.7
	1.0: 1.1	140	0.858	17.9	51.6	8.1
	1.0:1.2	140	0.838	16.8	53.5	7.5

The devices architecture is ITO/ZnO/active layer/MoO_3/Ag.

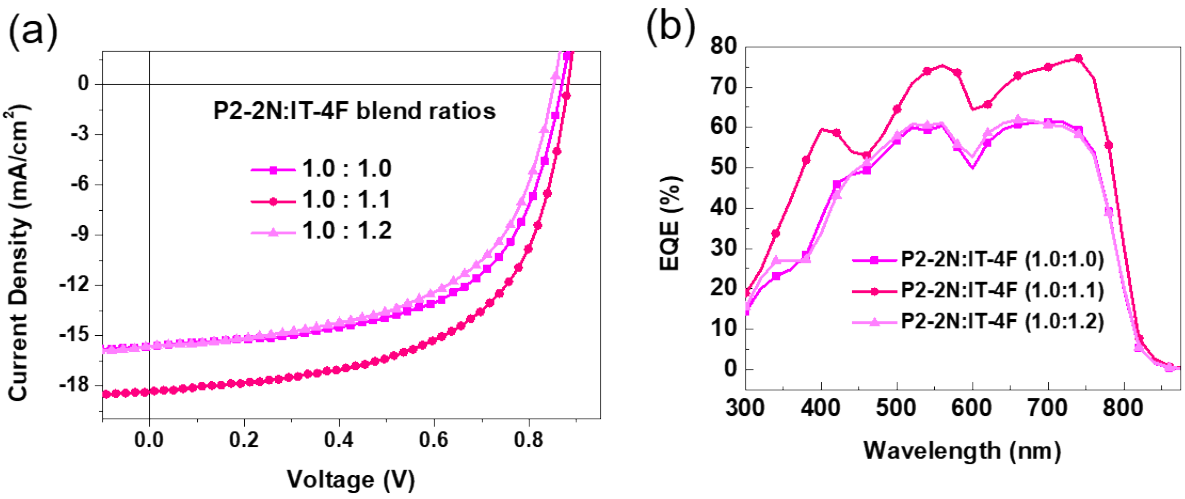

Figure S11. (a) *J-V* characteristics and (b) EQE corresponding profiles **P2-2N**:IT-4F based PSCs with different D:A blend ratios (CB/0.5 vol % DIO) under inverted device architecture ITO/ZnO/active layer/MoO3/Ag with thermal annealing 140 °C for 10 mins.

Table S2. Device characteristics of **P2-2N**:IT-4F (CB/0.5 vol % DIO) OSCs processed with different blend ratios under optimized device fabrication conditions.

Polymer	**Polymer:IT-4F blend ratio**	**Thermal annealing temperature [°C]**	V_{OC} **[V]**	J_{SC} **[mA/cm²]**	***FF*** **[%]**	**PCE [%]**
P2-2N	**1.0:0.8**	**140**	0.869	15.6	59.0	8.02
	1.0: 1:1	**140**	0.878	18.4	58.6	9.50
	1.0:1.2	**140**	0.852	15.6	56.5	7.53

The devices architecture is ITO/ZnO/active layer/MoO_3/Ag.

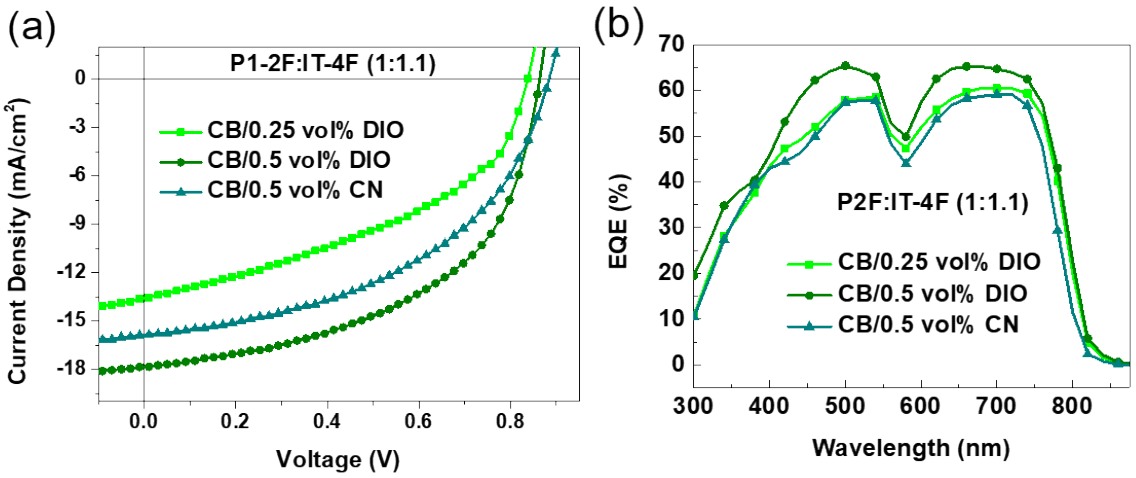

Figure S12. *J-V* and EQE characteristics of **P1-2F**:IT-4F (1:1) solar cell devices with different solvent additive conditions.

Table S3. Device characteristics of **P1-2F**:IT-4F (1:1.1)-based OSCs processed with different solvent additive under inverted device architecture ITO/ZnO/active layer/MoO_3/Ag with thermal annealing 140 °C for 10 mins.

Polymer	**Polymer:IT-4F blend ratio**	**Solvent/ additive**	V_{OC} **[V]**	J_{SC} **[mA/cm²]**	***FF*** **[%]**	**PCE [%]**
P1-2F	**1.0:1.0**	CB/0.25% DIO	0.838	15.4	39.5	5.1
		CB/0.5% DIO	0.858	17.9	51.6	8.1
		CB/0.5% CN	0.878	15.9	48.3	6.7

The devices architecture is ITO/ZnO/active layer/MoO_3/Ag.

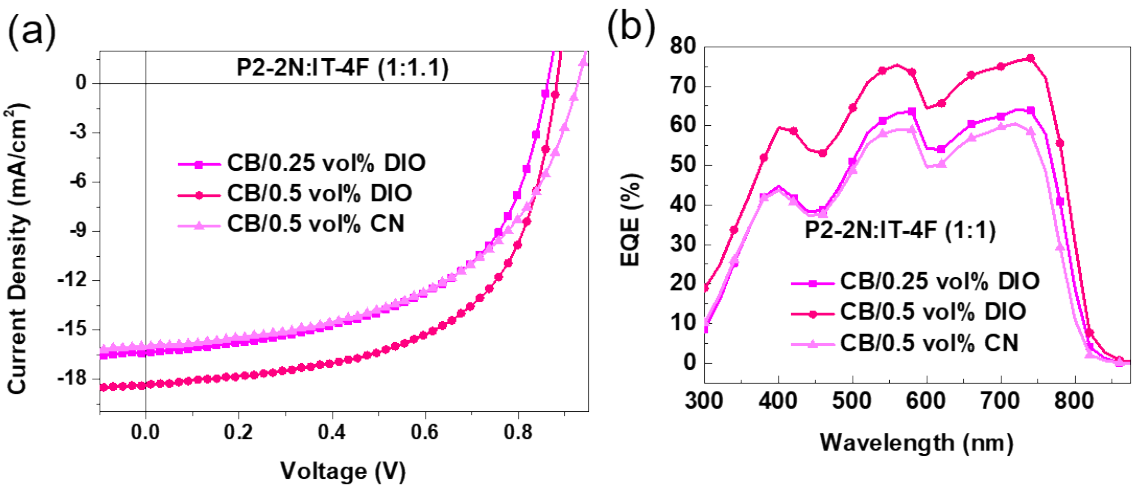

Figure S13. *J-V* and EQE characteristics of **P2-2N**:IT-4F (1:1) solar cell devices with different solvent additive conditions.

Table S4. Device characteristics of **P2-2N**:IT-4F (1:1.1)-based OSCs processed with different solvent additive under inverted device architecture ITO/ZnO/active layer/MoO_3/Ag with thermal annealing 140 °C for 10 mins.

Polymer	**Polymer:IT-4F blend ratio**	**Solvent/ additive**	V_{OC} **[V]**	J_{SC} **[mA/cm²]**	***FF*** **[%]**	**PCE [%]**
P2-2N	**1.0:1.0**	CB/0.25% DIO	0.858	16.4	55.5	7.9
		CB/0.5% DIO	0.878	18.4	58.6	9.5
		CB/0.5% CN	0.919	16.0	52.7	7.8

The devices architecture is ITO/ZnO/active layer/MoO_3/Ag.

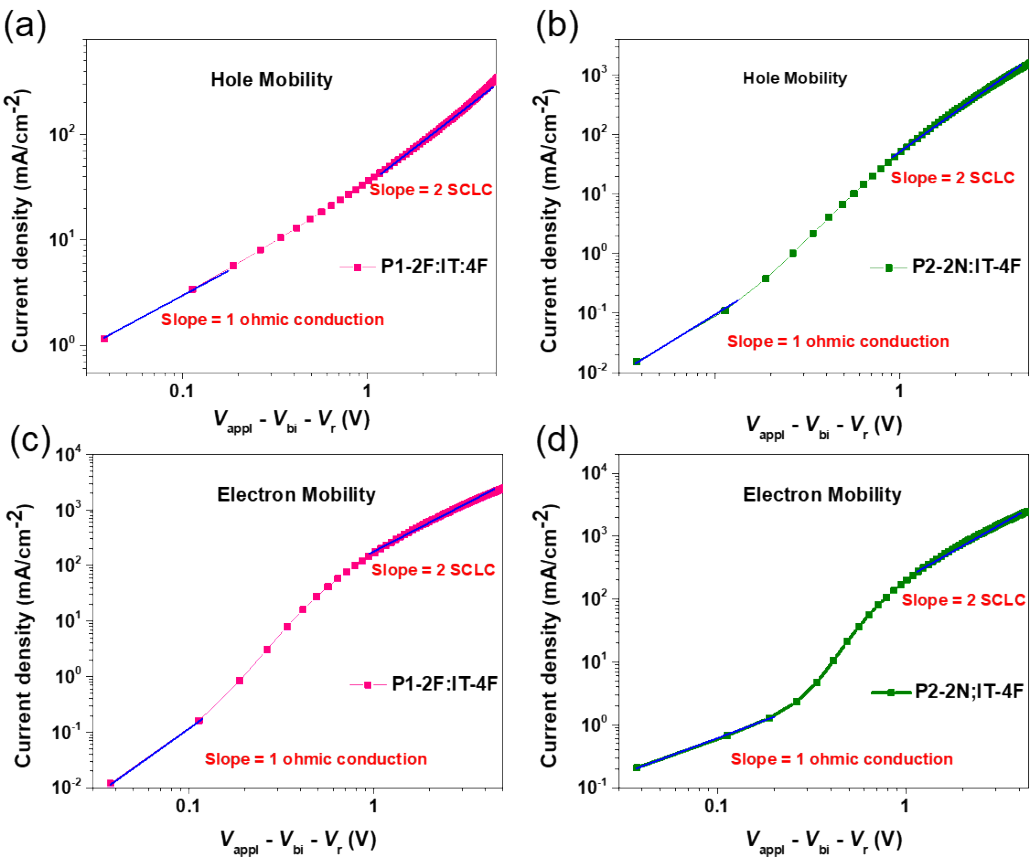

Figure S14. *J-V* characteristics of hole-only and electron-only devices for (a) and (c) **P1-2F**:IT-4F and (b) and (d) **P2-2N**:IT-4F blends were measured using the SCLC method.

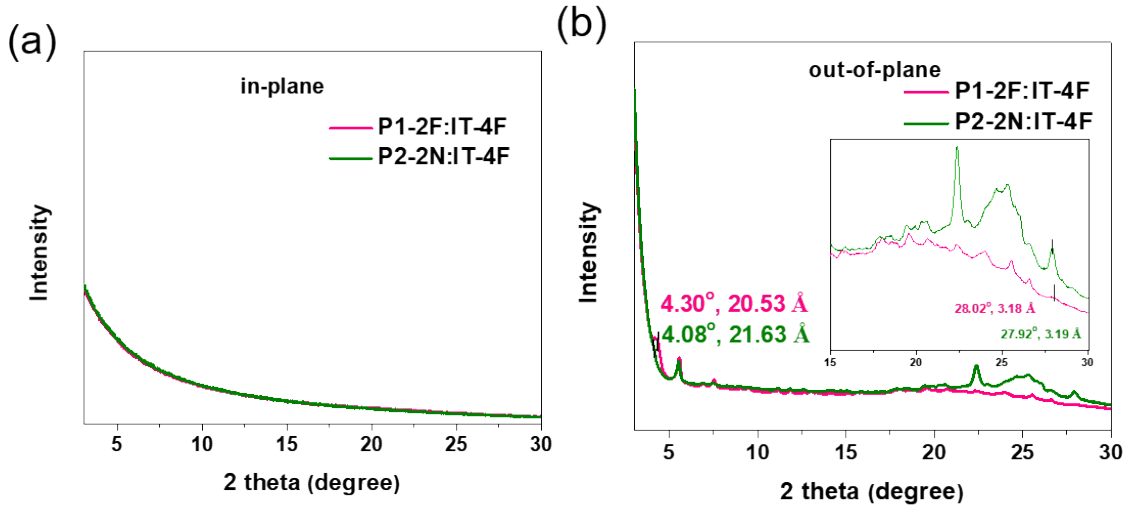

Figure S15. (a) In-plane (q_{xy}) and (b) out-of-plane (q_z) line cut profiles of the **P1-2F**:IT-4F and **P2-2N**:IT-4F blends obtained from the XRD.

References:

1. Duan, C.; Li, Z.; Pang, S.; Zhu, Y.-L.; Lin, B.; Colberts, F. J. M.; Leenaers, P. J.; Wang, E.; Sun, Z.-Y.; Ma, W.; Meskers, S. C. J.; Janssen, R. A. J., Improving Performance of All-Polymer Solar Cells Through Backbone Engineering of Both Donors and Acceptors. *Sol. RRL* **2018,** *2* (12), 1800247.
2. Lee, E. J.; Heo, S. W.; Han, Y. W.; Moon, D. K., An organic–inorganic hybrid interlayer for improved electron extraction in inverted polymer solar cells. *J. Mater. Chem. C* **2016,** *4* (13), 2463-2469.
3. Khizar ul, H.; A, K. M.; Xueyin, J.; Zhilin, Z.; Xiaowen, Z.; Liang, Z.; Jun, L., Estimation of electron mobility of n-doped 4, 7-diphenyl-1, 10-phenanthroline using space-charge-limited currents. *Journal of Semiconductors* **2009,** *30* (11), 114009.
4. Torabi, S.; Bahnamiri, F. J.; Van Severen, I.; Patil, S.; Havenith, R. W. A.; Chiechi, R. C.; Lutsen, L.; Vanderzande, D.; Cleij, T. J.; Hummelen, J. C.; Koster, L. J. A. In *Strategy for Enhancing the Electric Permittivity of Organic Semiconductors*, Light, Energy and the Environment, Canberra, 2014/12/02; Optica Publishing Group: Canberra, 2014; p JW6A.31.
5. Liu, M.; Yang, J.; Yin, Y.; Zhang, Y.; Zhou, E.; Guo, F.; Zhao, L., Novel perylene diimide-based polymers with electron-deficient segments as the comonomer for efficient all-polymer solar cells. *J. Mater. Chem. A* **2018,** *6* (2), 414-422.
6. Kini, G. P.; Park, H. S.; Jeon, S. J.; Han, Y. W.; Moon, D. K., A 2,5-difluoro benzene-based low cost and efficient polymer donor for non-fullerene solar cells. *Solar Energy* **2020,** *207*, 720-728.
7. Kini, G. P.; Choi, J. Y.; Jeon, S. J.; Suh, I. S.; Moon, D. K., Effects of incorporated pyrazine on the interchain packing and photovoltaic properties of wide-bandgap D–A polymers for non-fullerene polymer solar cells. *Polym. Chem.* **2019,** *10* (32), 4459-4468.